

PROFILES OF MATERIAL PROPERTIES IN INDUCTION-HARDENED STEEL DETERMINED THROUGH INVERSION OF RESONANT ACOUSTIC MEASUREMENTS[†]

W. L. Johnson,¹ S. A. Kim,¹ and S. J. Norton²

¹NIST, Materials Reliability Division, 325 Broadway, Boulder, CO 80305

²Geophex Ltd., 605 Mercury Street, Raleigh, NC 27603

ABSTRACT. Electromagnetic-acoustic measurements of resonant frequencies of induction-hardened steel shafts were used in an inverse calculation to determine parameters of the radial variations in the shear constant and density, including the effects of material variations and residual stress. Parameters determined for the profile of the shear constant were consistent with independent measurements on cut specimens and estimates of the acoustoelastic contribution. The profiles determined for material variations were close to those of the measured hardness.

INTRODUCTION

Over the past decade, efforts at establishing nondestructive methods for the determination of case depth in induction-hardened or carburized steel have included innovative electromagnetic-acoustic resonance (EMAR) techniques applied to cylindrical specimens. Johnson, Auld, and Alers [1] and Johnson and Alers [2] demonstrated that changes in the frequencies of axial-shear resonant modes are strongly correlated with case depth. The correlation of the destructively determined case depth with the frequency of one selected mode of a series of 63 induction-hardened automotive shafts was shown to have a standard deviation of 0.13 mm, which is on the order of the uncertainty in the destructive measurement itself [2]. As originally suggested by Johnson, Auld, and Alers [1], the systematic dependence of the penetration depth of axial-shear displacements also can be used to determine parameters of the profile through inversion of the measured frequency shifts without employing an empirical correlation. Hirao, Ogi, and Minami [3] successfully pursued this approach on induction-hardened shafts using a perturbation formulation that approximated the radial profiles of the shear constant and density as abrupt steps. Their results for the case depth determined from the resonant frequency of a single mode agree within 0.1 mm with destructive measurements. In the current report, we proceed beyond the work of Hirao, Ogi, and Minami [3] to explore the use of EMAR measurements for determining the width of the transitional region, in addition to the case depth in cylindrical specimens. We also introduce terms in the calculation that seek to approximate the effects of stress on the shear constant and density. To enable the determination of several parameters of the profiles, the inversion is performed using the

[†] Contribution of NIST. Not subject to copyright in the United States.

resonant frequencies of a series of modes. The use of more than one mode also eliminates the need to accurately measure the diameters of specimens.

EXPERIMENTAL TECHNIQUE

An EMAR transducer was employed with an array of twenty-six magnets of alternating polarity arranged around the circumference of a cylindrical specimen [1, 4]. A solenoid coil inside the array of magnets surrounded the specimen. A capacitor in parallel with the coil was used to bring the frequency of the electrical LC resonance into the range of the measurements and increase the magnitude of the currents in the coil during generation and detection. The coil was driven with a sinusoidal tone burst having a duration of 1-3 ms. This induced eddy currents in the specimen, produced Lorentz forces with the periodicity of the magnets, and excited axial-shear resonances with the same periodicity [1].

Approximate resonant frequencies were determined by monitoring the amplitude of the resonant ringdown while scanning the frequency. More accurate frequencies then were determined from linear fitting of the phase versus time following excitation at a frequency near each resonance [5]. Uncertainties in the final values are on the order of 1 part in 10^5 .

Conventional resonant ultrasound spectroscopy (RUS) was used in conjunction with Ritz analysis to determine elastic constants of parallelepiped specimens. These measurements employed contacting piezoelectric transduction.

THEORY

Because of the direction and periodicity of the forces, the EMAR transducer couples primarily to resonant shear modes with displacements in the axial direction, thirteen periods around the circumference, and radial variations in phase and amplitude that are dependent on the frequency. For the most strongly excited modes, the axial variations in phase and amplitude are small relative to the azimuthal and radial variations, so that the displacements are closely approximated by those of pure axial-shear modes [6]:

$$\vec{u} = \hat{z}u_0 J_n(\eta\bar{r}) \cos(n\theta) \cos(\omega_0 t), \quad (1.a)$$

$$\omega_0 = \eta v / a, \quad (1.b)$$

where θ is the azimuthal angle, \hat{z} is the axial unit vector, a is the radius of the cylinder, \bar{r} is the radial coordinate divided by a , v is the shear velocity, n is an integer, and J_n is the Bessel function of order n . The allowed values for η are determined by the boundary condition of zero stress at the surface [6]. For $n = 13$, the first ten values of η are 14.928374, 19.883224, 23.819389, 27.474340, 30.987394, 34.414546, 37.784379, 41.113512, 44.412455, and 47.688253.

Hirao, Ogi, and Minami [3] and Hirao and Ogi [7] have presented a perturbation equation for the fractional shift in frequency resulting from small radial variations in the shear constant μ and density ρ . Here, we present a slightly revised version of this equation,

$$\frac{\Delta\omega}{\omega_0} = \frac{\int_0^1 \left\{ \left[\frac{\Delta\mu(\bar{r})}{2\mu_0} \right] \left[J_{n-1}^2(\eta\bar{r}) + J_{n+1}^2(\eta\bar{r}) \right] - \left[\frac{\Delta\rho(\bar{r})}{\rho_0} \right] \left[J_n^2(\eta\bar{r}) \right] \right\} \bar{r} d\bar{r}}{2 \int_0^1 J_n^2(\eta\bar{r}) \bar{r} d\bar{r}}, \quad (2)$$

which differs in the corrected factor of 2 (instead of 4) dividing the first term in the numerator. In this equation, μ_0 and ρ_0 are the shear modulus and density at the center of the cylinder. $\Delta\mu(\bar{r})$ and $\Delta\rho(\bar{r})$ are the shifts in shear modulus and density relative to μ_0 and ρ_0 . $\Delta\omega$ is the shift in resonant frequency of an axial-shear mode relative to that of an isotropic cylinder with shear modulus and density equal to μ_0 and ρ_0 .

If measurements are performed of the shifts in axial-shear frequencies of a case-hardened shaft relative to an isotropic unhardened shaft, Eq. (2) can be incorporated in a nonlinear fitting routine to determine parameters for specified functional forms of $\Delta\mu(\bar{r})$ and $\Delta\rho(\bar{r})$. If a particular relationship between the hardness and μ and/or ρ (in the simplest case, a proportionality) is assumed, then the shape of the hardness profile can be inferred.

SPECIMENS

The specimens investigated in this study are sections of automotive drive shafts. The material is fine-grained hot-rolled SAE 1050 steel with a composition (in weight percent) of 0.48-0.55 C, 0.9-1.1 Mn, 0.15-0.30 Si, 0.3 Al, <0.050 S, <0.04 P, <0.10 Ni, <0.12 Cr, <0.05 Mo, and <0.18 Cu. As depicted in Fig. 1, each specimen has a short section where grooves have been machined around the circumference and a set of longitudinal splines at one end. The original shaft from which each specimen was cut extended 3 cm beyond the end with the splines and 21 cm beyond the other end of the specimen. The EMAR transducer was centered on the 69-mm-long region with a diameter of 23.8 mm.

Two induction-hardened specimens were studied with EMAR. Microficial hardness measurements of the end of each specimen without the splines were supplied by the manufacturer, and these were converted to the more familiar Rockwell-C scale. The radii of the transitions in hardness were approximately 7.5 mm (specimen B417) and 6.0 mm (specimen B560). Another specimen, B500, was annealed to remove the hardening and served as a reference for the shifts in frequencies of the hardened specimens. The use of a reference having the same geometry as the induction-hardened specimens also compensates for slight shifts in frequency that arise from the axial dependence of the modal displacement patterns. Small rectangular parallelepipeds were cut from the core and outer region of similar induction-hardened specimens to determine elastic constants and density of fully hardened and soft material using RUS.

RESULTS

Ritz analysis of RUS measurements performed on the parallelepiped specimens determined shear constants for waves polarized in the axial direction to be 82.10 ± 0.05 GPa in the unhardened material and 78.9 ± 0.2 GPa in the hardened material. This corresponds to a fractional difference of $(-3.9 \pm 0.3) \times 10^{-2}$ relative to the unhardened

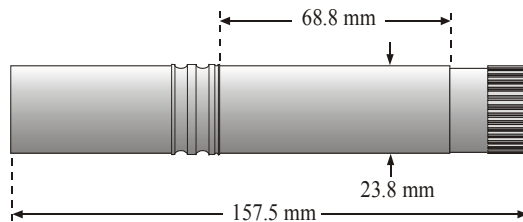


FIGURE 1. Section of an induction-hardened automotive drive shaft.

material. The Young moduli were determined to be approximately 211 GPa in the unhardened material and 204 GPa in the hardened material, and the Poisson ratio was determined to be approximately 0.29 in both specimens. More detailed results from the RUS measurements will be presented elsewhere. The measured densities were $7.709 \pm 0.001 \text{ g/cm}^3$ for the hardened material and $7.835 \pm 0.002 \text{ g/cm}^3$ for the unhardened material, corresponding to a fractional difference of $(-1.61 \pm 0.03) \times 10^{-2}$.

The discussion presented here of EMAR measurements and inverse calculations will focus on specimen B417 and return to specimen B560 only for final results. Intermediate results for the two specimens are qualitatively similar.

Measurements of the fractional shift in resonant axial-shear frequencies of specimen B417 relative to the reference specimen B500 are shown in Fig. 2. The systematic increase in $\Delta\omega/\omega_0$ with increasing mode index is a result of the displacements extending more deeply into the specimen at higher frequencies [1] and the shear modulus being higher in the unhardened core.

To extract information on the radial variations of $\Delta\mu/\mu_0$ and $\Delta\rho/\rho_0$ from the measurements shown in Fig. 2, general functional forms must be assumed. We begin by assuming that these profiles have the form of simple displaced hyperbolic tangents: $\Delta\mu\{1 + \tanh[(r-B)/W]\}$ and $\Delta\rho\{1 + \tanh[(r-B)/W]\}$, respectively. Figure 2 shows the result of Gauss-Newton fitting using such functions in Eq. (2). An adjustable constant also is added to Eq. (2) to compensate for slight differences in radius, temperature, μ_0 , and ρ_0 of specimens B417 and B500. The spatial profiles corresponding to the fit in Fig. 2 have $B = 7.11 \text{ mm}$, $W = 0.15 \text{ mm}$, $\Delta\mu = -1.57 \times 10^{-2}$, and $\Delta\rho = 1.64 \times 10^{-3}$. The value obtained for B is to be compared with a value of 7.45 mm for the radius determined by directly fitting the hardness measurements (described below). The value for $\Delta\mu$ is of the same order of magnitude as the fractional difference of -3.9×10^{-2} between hardened and unhardened parallelepiped specimens determined from the RUS measurements. However, the value for $\Delta\rho$ is an order of magnitude smaller and opposite in sign to the value of -1.6×10^{-2} determined from RUS.

The small positive value obtained for $\Delta\rho$ indicates that the general form of the assumed profiles is incorrect. In fact, residual stress can be expected to have a significant effect on

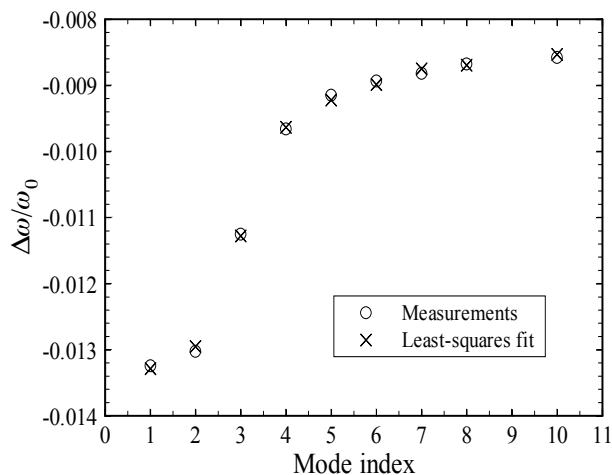


FIGURE 2. Fractional shift in axial-shear resonant frequencies of B417 relative to B500 and a fit of these data to Eq. (2) assuming displaced hyperbolic tangent profiles for μ and ρ .

both μ and ρ . Prask and Choi [8] performed neutron diffraction measurements on a similar induction-hardened steel specimen having a diameter of 40 mm and a case depth of approximately 4 mm. Their results show that axial, azimuthal (hoop), and radial stresses are each lower at the surface than at the center. The magnitudes of the changes in these stress components were found to be approximately 900 MPa, 1300 MPa, and 200 MPa, respectively.

For the purposes of estimating the effects of stress, we neglect the radial component and assume the axial and hoop components are equal. With a 1100 MPa drop in axial and hoop stresses between the center and the surface, the stress-induced component of $\Delta\rho/\rho_0$ is estimated to be 5×10^{-3} . Using third-order elastic constants measured by Smith, Stern, and Stephens [9] and expressions for the acoustoelastic effect presented by Toupin and Bernstein [10], the stress-induced component of $\Delta\mu/\mu_0$ is estimated to be 2×10^{-2} . Note that the stress-induced changes are opposite in sign to those associated with microstructural differences in hardened and unhardened material, which are reflected in the measurements on parallelepiped specimens.

To approximate the effects of residual stress, additional terms are added to the functions used for the profiles:

$$\frac{\Delta\mu}{\mu_0} = \Delta_{\mu 1} \left[1 + \tanh\left(\frac{r - B_1}{W_1}\right) \right] + \Delta_{\mu 2} \left[1 + \tanh\left(\frac{r - B_2}{W_2}\right) \right], \quad (3)$$

$$\frac{\Delta\rho}{\rho_0} = \Delta_{\rho 1} \left[1 + \tanh\left(\frac{r - B_1}{W_1}\right) \right] + \Delta_{\rho 2} \left[1 + \tanh\left(\frac{r - B_2}{W_2}\right) \right]. \quad (4)$$

The first term in each of these expressions is intended to represent the contribution from variations in phase and microstructure, and the second is intended to represent the contribution from residual stress. Because of the large number of adjustable parameters, the use of Eqs. (3) and (4) in Eq. (2) leads to a number of unrealistic local minima for $\Delta\omega/\omega$, and constraints must be imposed in the fitting algorithm. The constraint that we have employed involves first performing the calculation with $\Delta_{\mu 1}$ fixed at the value obtained from the RUS measurements, -3.9×10^{-2} , and then using the parameters obtained from this calculation as initial guesses in a calculation that allows $\Delta_{\mu 1}$ to vary.

Figures 3 and 4 show the results of such a calculation for specimens B417 and B560. These figures also show direct least-squares fits of the hardness data to a displaced hyperbolic tangent, $\Delta_h \{1 + \tanh[(r - B_h)/W_h]\} + H_0$, where Δ_h , B_h , W_h , and H_0 are adjustable parameters. To enable comparisons of the profiles, the y -axes are scaled such that 0 on the right axis matches H_0 on the left axis, and 1 on the right axis matches $\Delta_h + H_0$ on the left axis. The values obtained for the parameters of Eqs. (3) and (4) are presented in Table 1. From the direct fits of hardness, values obtained for B417 are $B_h = 7.45$ mm and $W_h = 0.71$ mm, and values obtained for B560 are $B_h = 5.98$ mm and $W_h = 0.84$ mm.

In several respects, the results of the inverse calculations presented in Table 1 are consistent with expectations. Since the first terms in Eqs. (3) and (4) represent the effects of material differences, it is reasonable to expect that these terms will have approximately the same radial dependence as the hardness. Consistent with this assumption, B_1 and W_1 determined by the inverse calculation are close to the values obtained from the direct fit of hardness; $B_1 - B_h$ is -0.38 mm for B417 and 0.14 mm for B560. One should note, again, that the hardness was measured in a region that is different than that of the acoustic excitation. Therefore, the differences in B_1 and B_h may reflect actual differences in case depth in the two regions. The fact that W_2 is determined through inversion to be greater than W_1 is

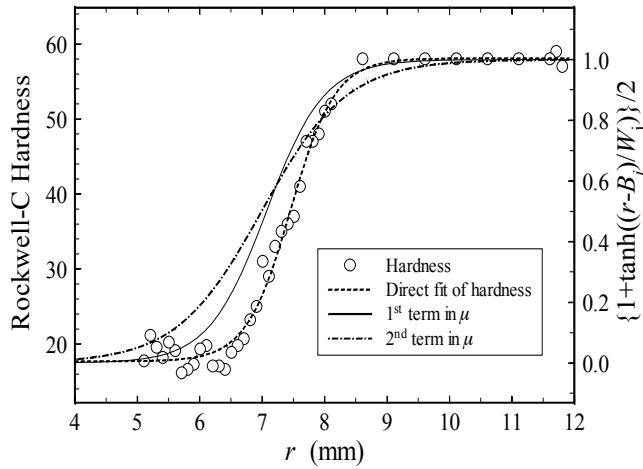


FIGURE 3. Specimen B417. Hardness measurements, a direct fit of the hardness, and the results of an inverse calculation using measured frequencies in Eqs. (2)-(4).

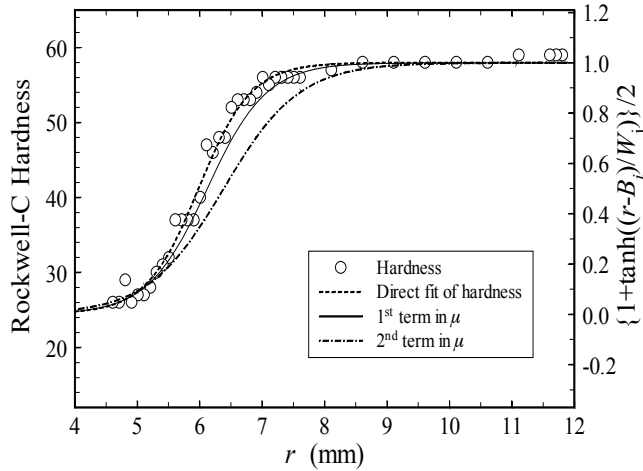


FIGURE 4. Specimen B560. Hardness measurements, a direct fit of the hardness, and the results of an inverse calculation using measured frequencies in Eqs. (2)-(4).

TABLE 1. Parameters determined by fitting the frequency shifts of specimens B417 and B560 to Eq. (2) with the profiles of Eqs. (3) and (4).

	B417	B560
$\Delta_{\mu 1}$	-3.91×10^{-2}	-3.35×10^{-2}
$\Delta_{\mu 2}$	2.62×10^{-2}	2.50×10^{-2}
$\Delta_{\rho 1}$	1.14×10^{-2}	2.44×10^{-2}
$\Delta_{\rho 2}$	-8.11×10^{-3}	-1.65×10^{-2}
B_1 (mm)	7.07	6.12
W_1 (mm)	0.92	0.95
B_2 (mm)	6.99	6.38
W_2 (mm)	1.36	1.21

consistent with the results of Prask and Choi [8], which show a broader transition for the stress than the hardness. The values obtained for $\Delta\mu_1$ are consistent with the expectation from RUS measurements, and fact that this parameter is found to be somewhat lower for B560 than for B417 may be a result of slight hardening of the core of B560, which is suggested by the direct fit of the hardness (Fig. 4). The values obtained for $\Delta\mu_2$ are close to our estimate of 2×10^{-2} for the acoustoelastic contribution.

Although all of the parameters for the dominant terms in the fit [both contributions to $\Delta\mu/\mu_0$ in Eq. (3)] are consistent with expectations, parameters obtained for the profiles of $\Delta\rho/\rho_0$ are still implausible. The signs of the values of $\Delta\rho_1$ and $\Delta\rho_2$ obtained for both specimens are opposite to those expected from the measurements on parallelepipeds and the estimated effect of stress. Therefore, the assumed functional forms of the profiles remain, in some respect, inaccurate. One factor that has not been incorporated in the model is the difference in acoustoelastic coefficients of the hardened and unhardened materials.

CONCLUSION

This report presents the first inverse calculations seeking to determine hardness profiles from simultaneous fitting of the frequency shifts of a series of resonant axial-shear modes, including the effects of variations in material (microstructure and phase) and residual stress. The calculations convincingly determine contributions to the spatial profile of μ arising from variations in material and stress. The profile determined for material variations closely approximates that of the hardness.

ACKNOWLEDGMENTS

We thank Ken White of Bigfoot Enterprises for supplying specimens and hardness data and thank Dr. Patrick Purtscher for annealing one of the specimens. We also thank Dr. Henry Prask and Dr. Hirotosugu Ogi for several helpful discussions.

REFERENCES

1. W. Johnson, B. A. Auld, and G. A. Alers, in *Review of Progress in Quantitative Nondestructive Evaluation, Vol 13*, eds. D. O. Thompson and D. E. Chimenti. Plenum, New York, (1994), p. 1603.
2. W. Johnson and G. A. Alers, in *Wave Propagation and Emerging Technologies*, AMD-Vol. 188, eds. V. K. Kinra, R. J. Clifton, and G. C. Johnson (Am. Soc. Mech. Eng., New York, 1994), p. 61.
3. M. Hirao, H. Ogi, and Y. Minami, in *Nondestructive Characterization of Materials, Vol. 10* (Elsevier, Tokyo, 2001), p. 379.
4. W. Johnson, B. A. Auld, and E. Segal, *J. Acoust. Soc. Am.*, **100**, 285 (1996).
5. W. Johnson, *J. Phys. IV* (Suppl. to *J. Phys. III*, **6**), C8-849 (1996).
6. A. C. Eringen and E. S. Şuhubi, *Elastodynamics*, (Academic, New York, 1975), Vol. 2.
7. M. Hirao and H. Ogi, *EMATs for Science and Industry: Noncontacting Ultrasonic Measurements* (Kluwer, Boston, 2003).
8. H. J. Prask and C. S. Choi, in *Measurement of Residual and Applied Stress Using Neutron Diffraction*, eds. M. T. Hutchings and A. D. Krawitz (Kluwer, Boston, 1992), p. 1.
9. R. T. Smith, R. Stern, and R. W. B. Stephens, *J. Acoust. Soc. Am.*, **40**, 1002 (1966).
10. R. A. Toupin and B. Bernstein, *J. Acoust. Soc. Am.*, **33**, 1002 (1961).